ADVANCED FUNCTIONAL MATERIALS
www.afm-journal.de

Gelatin Methacryloyl-Based Tactile Sensors for Medical Wearables

Zhikang Li, Shiming Zhang, Yihang Chen, Haonan Ling, Libo Zhao,* Guoxi Luo, Xiaochen Wang, Martin C. Hartel, Hao Liu, Yumeng Xue, Reihaneh Haghniaz, KangJu Lee, Wujin Sun, HanJun Kim, Junmin Lee, Yichao Zhao, Yepin Zhao, Sam Emaminejad, Samad Ahadian, Nureddin Ashammakhi, Mehmet R. Dokmeci, Zhuangde Jiang, and Ali Khademhosseini**

Gelatin methacryloyl (GelMA) is a widely used hydrogel with skin-derived gelatin acting as the main constituent. However, GelMA has not been used in the development of wearable biosensors, which are emerging devices that enable personalized healthcare monitoring. This work highlights the potential of GelMA for wearable biosensing applications by demonstrating a fully solution-processable and transparent capacitive tactile sensor with microstructured GelMA as the core dielectric layer. A robust chemical bonding and a reliable encapsulation approach are introduced to overcome detachment and water-evaporation issues in hydrogel biosensors. The resultant GelMA tactile sensor shows a high-pressure sensitivity of 0.19 kPa^{-1} and one order of magnitude lower limit of detection (0.1 Pa) compared to previous hydrogel pressure sensors owing to its excellent mechanical and electrical properties (dielectric constant). Furthermore, it shows durability up to 3000 test cycles because of tough chemical bonding, and long-term stability of 3 days due to the inclusion of an encapsulation layer, which prevents water evaporation (80% water content). Successful monitoring of various human physiological and motion signals demonstrates the potential of these GelMA tactile sensors for wearable biosensing applications.

Dr. Z. Li, Dr. S. Zhang, Y. Chen, H. Ling, X. Wang, M. C. Hartel, Dr. H. Liu, Y. Xue, Dr. R. Haghniaz, Dr. K. Lee, Dr. W. Sun, Prof. H. Kim, Dr. J. Lee, Prof. S. Ahadian, Prof. N. Ashammakhi, Prof. M. R. Dokmeci, Prof. A. Khademhosseini
Department of Bioengineering
University of California-Los Angeles
Los Angeles, CA 90095, USA
E-mail: szhang@eee.hku.hk; khademh@terasaki.org

Dr. Z. Li, Dr. S. Zhang, Y. Chen, H. Ling, X. Wang, M. C. Hartel, Dr. H. Liu, Y. Xue, Dr. R. Haghniaz, Dr. K. Lee, Dr. W. Sun, Prof. H. Kim, Dr. J. Lee, Prof. S. Ahadian, Prof. N. Ashammakhi, Prof. M. R. Dokmeci, Prof. A. Khademhosseini
Center for Minimally Invasive Therapeutics (C-MIT)
University of California-Los Angeles
Los Angeles, CA 90095, USA

Dr. Z. Li, Dr. S. Zhang, Y. Chen, H. Ling, X. Wang, M. C. Hartel, Dr. H. Liu, Y. Xue, Dr. R. Haghniaz, Dr. K. Lee, Dr. W. Sun, Prof. H. Kim, Dr. J. Lee, Y. Zhao, Prof. S. Ahadian, Prof. N. Ashammakhi, Prof. M. R. Dokmeci, Prof. A. Khademhosseini
California NanoSystems Institute
University of California-Los Angeles
Los Angeles, CA 90095, USA

Dr. Z. Li, Prof. L. Zhao, Dr. G. Luo, Prof. Z. Jiang
School of Mechanical Engineering
Xi'an Jiaotong University
Xi'an 710049, China
E-mail: libozhao@xjtu.edu.cn

The ORCID identification number(s) for the author(s) of this article can be found under https://doi.org/10.1002/adfm.202003601.

DOI: 10.1002/adfm.202003601

Dr. Z. Li, Prof. L. Zhao, Dr. G. Luo, Prof. Z. Jiang
State Key Laboratory for Manufacturing Systems Engineering
Xi'an Jiaotong University
Xi'an 710049, China

Dr. Z. Li, Prof. L. Zhao, Dr. G. Luo, Prof. Z. Jiang
International Joint Laboratory for Micro/Nano Manufacturing and Measurement Technologies
Xi'an Jiaotong University
Xi'an 710049, China

Dr. S. Zhang, Dr. R. Haghniaz, Dr. K. Lee, Dr. W. Sun, Prof. H. Kim, Dr. J. Lee, Prof. S. Ahadian, Prof. M. R. Dokmeci, Prof. A. Khademhosseini
Terasaki Institute for Biomedical Innovation
Los Angeles, CA 90024, USA

H. Ling
Department of Mechanical and Aerospace Engineering
University of California-Los Angeles
Los Angeles, CA 90095, USA

X. Wang
School of Mechanical Engineering
Zhejiang University of Technology
Hangzhou, Zhejiang 310000, China

Dr. H. Liu
Ministry of Education Key Laboratory of Biomedical Information Engineering
Xi'an Jiaotong University
Xi'an 710049, China

Y. Xue
Frontier Institute of Science and Technology
Xi'an Jiaotong University
Xi'an 710049, China

1. Introduction

Wearable tactile sensors have been in high demand in fast-growing fields, such as personalized healthcare, human-machine interfaces, and the internet of things because they allow real-time, low-cost, and long-term monitoring of human physiological signals. In the past decade, various wearable tactile sensors have been developed, including to monitor pressure, strain, vibration, temperature, and humidity.[1,2] Among these sensors, pressure sensors are of great importance and widely investigated due to their ability to sense human physical and physiological signals such as gentle touch (<10 kPa), wrist pulse, blood pressure, heart rate, and respiration rate.[3–5] However, to date, the majority of developed wearable pressure sensors are based on elastomers such as polydimethylsiloxane (PDMS), polyurethane (PU), VHB, and Ecoflex.[6–11] The mechanical mismatch between these elastomers (1 MPa–1 GPa) and human tissue (≈10 kPa), as well as issues of biocompatibility, limits their future practical applications.[12,13]

Compared to elastomers, hydrogels, consisting of 3D cross-linked polymers, are considered promising in developing next-generation wearable pressure sensors because of their intrinsic biocompatibility and low Young's modulus.[13,14] Therefore, increasing efforts are being devoted to developing hydrogel-based wearable pressure sensors. For instance, Yin et al.[15] developed a polyacrylamide (PAAm) hydrogel pressure sensor based on the principle of electrical-double-layer, demonstrating a pressure sensitivity of 2.33 kPa^{-1} in 0–3 kPa. Wei et al.[16] and Wu et al.[17] exploited polyvinyl alcohol (PVA) and polyacrylic acid/alginate hydrogels based wearable ionic pressure sensors, respectively, showing corresponding pressure sensitivities of 0.033 and 0.17 kPa^{-1}. Dong et al.[18] demonstrated a wearable piezoresistive pressure sensor with pressure sensitivity of 0.05 kPa^{-1} using a PVA-PAAm hydrogel. Besides, various other hydrogels, such as PAAm composite hydrogels,[19] alginate composite hydrogels,[20] gelatin hydrogels,[21] and Fmoc-FF-PAni composite hydrogels,[22] were also synthesized to construct wearable pressure sensors. These studies demonstrated the feasibility of using hydrogels in developing wearable pressure sensors. However, there are still unsolved challenges in hydrogel-based wearable biosensors, such as water evaporation, weak interface bonding, and the lack of cost-effective fabrication techniques for large-scale production.

Y. Zhao, Prof. S. Emaminejad
Department of Electrical and Computer Engineering
University of California-Los Angeles
Los Angeles, CA 90095, USA
Y. Zhao
Department of Materials Science and Engineering
University of California-Los Angeles
Los Angeles, CA 90095, USA
Prof. N. Ashammakhi, Prof. M. R. Dokmeci, Prof. A. Khademhosseini
Department of Radiology
University of California-Los Angeles
Los Angeles, CA 90095, USA
Prof. A. Khademhosseini
Department of Chemical and Biomolecular Engineering
University of California-Los Angeles
Los Angeles, CA 90095, USA

Gelatin methacryloyl (GelMA) is a hydrogel obtained by conjugating methacrylic anhydride (MA) to gelatin, which is derived directly from the skin. It has superior biocompatibility compared to other artificial hydrogels and has been widely used in cell culture, soft tissue adhesives, and implantations.[23,24] Additionally, GelMA has similar Young's modulus to human tissue, which can contribute to excellent bio-mechanical matching at electronic-tissue interfaces. Its mechanical properties are also highly tunable, enabling GelMA-based devices to meet different mechanical stiffness requirements in practical applications. Importantly, GelMA has excellent robustness, allowing the recovery to its original shape after compressing (Figure S1, Video S1, Supporting Information). Furthermore, GelMA has good transparency, making it an ideal candidate for developing fully transparent bioelectronics. The above facts indicate GelMA as a promising hydrogel for developing highly sensitive, skin-conformal, biocompatible, and transparent wearable pressure sensors. However, GelMA-based wearable pressure sensors have been rarely reported so far.

Herein, we demonstrate the successful development of GelMA-based wearable capacitive tactile sensors for monitoring human physiological signals (**Figure 1**). We report the first investigation into the electrical property (dielectric constant) of GelMA hydrogels under different synthesis conditions. Based on its tailorable mechanical and electrical properties, we demonstrate the feasibility of GelMA in developing highly-sensitive and performance-tunable pressure sensors with a layer-by-layer stacked capacitive assembly. Sequentially, a fully solution-processable and transparent GelMA-based pressure sensor structure is proposed, with conducting polymer PEDOT:PSS as transparent electrodes and PDMS/GelMA/PDMS as dielectric layers. In this unique design, GelMA serves as the core dielectric layer; PDMS serves as an insulator between the GelMA dielectric layer and electrodes, and also as an encapsulation layer to prevent water evaporation of GelMA. A chemical bonding method is further introduced to solve the delamination issue between GelMA and elastomers. The resultant GelMA pressure sensor is structurally robust because of the enhanced interface bonding and fully transparent because of the optical transparency of each component. Compared to previously reported hydrogel-based pressure sensors, it shows a higher sensitivity and a lower limit of detection (LOD).[25–28] Furthermore, our GelMA pressure sensor shows high durability over 3000 cyclic tests, and long-term stability up to 3 days' exposure to air, demonstrating the robustness of the device structure and the reliability of the encapsulation. Furthermore, we demonstrate successful monitoring of human physiological signal, pulse, and vocal cord vibration using the developed GelMA hydrogel tactile sensors, encouraging their practical use in medical wearable applications.

2. Results and Discussion

2.1. Mechanical Properties and Relative Permittivity Characterization of GelMA Hydrogels

Material properties of the dielectric layer, such as Young's modulus, viscous modulus, and relative permittivity, are key

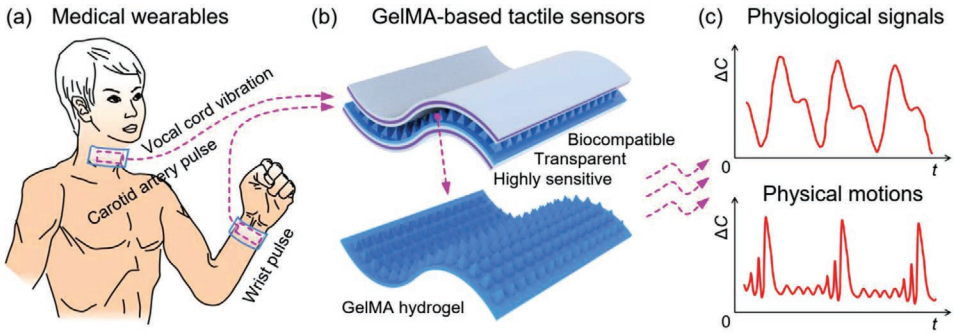

Figure 1. Schematic of GelMA hydrogel-based capacitive tactile sensors and their medical wearable applications. GelMA hydrogel-based sensitive, biocompatible, and transparent tactile sensors are developed and used on the human body to real-time monitor various physiological signals for medical diagnostics. a) Typical on-body use of GelMA hydrogel-based capacitive tactile sensors, such as vocal cord vibration detection, language recognition, wrist and carotid artery pulses monitoring. b) GelMA hydrogel-based capacitive tactile sensors. c) Real-time detection of various physical motions and physiological signals.

parameters influencing the performances of capacitive pressure sensors.[29,30] For GelMA hydrogels, their mechanical property and relative permittivity are dependent on several variables: The degree of substitution (DS) of MA, the concentration of GelMA, the concentration of photoinitiator (PI), ultraviolet (UV) light intensity, and UV crosslinking time.[31] To date, the effects of these parameters on their viscous modulus and electrical permittivity have been rarely investigated,[32–35] which are directly related to the response time and pressure sensitivity of the capacitive pressure sensor, respectively. We first studied the dependence of modulus and relative permittivity of GelMA hydrogels with respect to UV crosslinking time by fixing the other variables. That was to determine the time required for complete chemical crosslinking and to obtain stable mechanical and electrical properties.[36] Subsequently, we investigated their dependence on MA volume (DS of MA) and GelMA concentration at the determined crosslinking conditions (PI concentration, UV light intensity, and crosslinking time), revealing the tailorable range of the modulus and relative permittivity.

The results of the mechanical and electrical properties of the GelMA hydrogels under different synthesis conditions are shown in **Figure 2**. The storage modulus increased, while the loss modulus and relative permittivity decreased with time and reached a plateau at greater than 300 s for different PI concentrations of GelMA hydrogels, indicating the chemical crosslinking was completed (Figure 2a). In the following experiments, we investigated the effects of MA volume (DS of MA) and GelMA concentration on both properties of the GelMA hydrogels. We observed that the storage modulus of GelMA hydrogels increased from 4.6 to 15.9 kPa when increasing the MA volume from 2% to 20% (Figure 2b-i), and from 1.2 to 15.9 kPa when increasing the GelMA concentration from 10% to 20% (Figure 2c-i). The loss modulus showed no obvious dependence on MA volume and GelMA concentration (≈0.3 kPa in Figure 2b-i and ≈0.2 kPa in Figure 2c-i), indicating their negligible influence on the response time. The relative permittivity showed a negligible change with increased MA volume, but a distinct decrease (39–16) with increased GelMA concentrations (10%–20%), which could be attributed to the lower water content in the highly cross-linked GelMA hydrogel (Figure 2b-ii,c-ii). The relative permittivity was also significantly affected by the increased frequency, that is, 24 at 10 kHz and 12 at 500 kHz (Figure 2d). Both Young's modulus (1.2–15.9 kPa) and relative permittivity (16–39) of GelMA hydrogels could be tailored in a wide range, highlighting their superior tunability. The Young's modulus of GelMA hydrogels is two orders of magnitude lower (Figure 2e), and their electrical permittivity is three times higher (Figure 2f) than those of their elastomeric competitors.[37–42] These outstanding properties indicate the great potential of GelMA hydrogels in developing high-performance capacitive pressure sensors.

2.2. Performance and Tunability Evaluation of GelMA Hydrogels for Capacitive Pressure Sensors

To evaluate the potential of using GelMA hydrogels to develop pressure sensors, we assembled a capacitive pressure sensor with a layer-by-layer stacking method (**Figure 3**a-i). The device performance was compared to that of a reference device fabricated with PDMS as the dielectric layer in a pressure range between 0 and 84 kPa (Figure 3a-ii). As shown in Figure 3b, the stacked GelMA-based pressure sensor showed a pressure sensitivity of 6.5×10^{-3} kPa^{-1} in the pressure range of 0–17 kPa, which was one order of magnitude higher than that of the PDMS-based device. The sensitivity decreased to 8.7×10^{-4} kPa^{-1} in the pressure range of 25–84 kPa, which was attributable to the reduced deformability of GelMA hydrogels under high pressure. These results indicate that, compared with elastomers, GelMA hydrogels enable a significant improvement in pressure sensitivity. The pressure sensitivity can be further increased to approach its theoretical limit (two orders of magnitude higher than that of PDMS-based pressure sensors, shown in Figure S2b, Supporting Information) by optimizing the stacked pressure sensor and experimental testing approach.

The sensitivity of GelMA pressure sensors can be tuned by changing the MA volume and GelMA concentration. The pressure sensitivity can be increased by decreasing MA volume and GelMA concentrations, which is reasonable because of the decrease in Young's modulus. For the studied

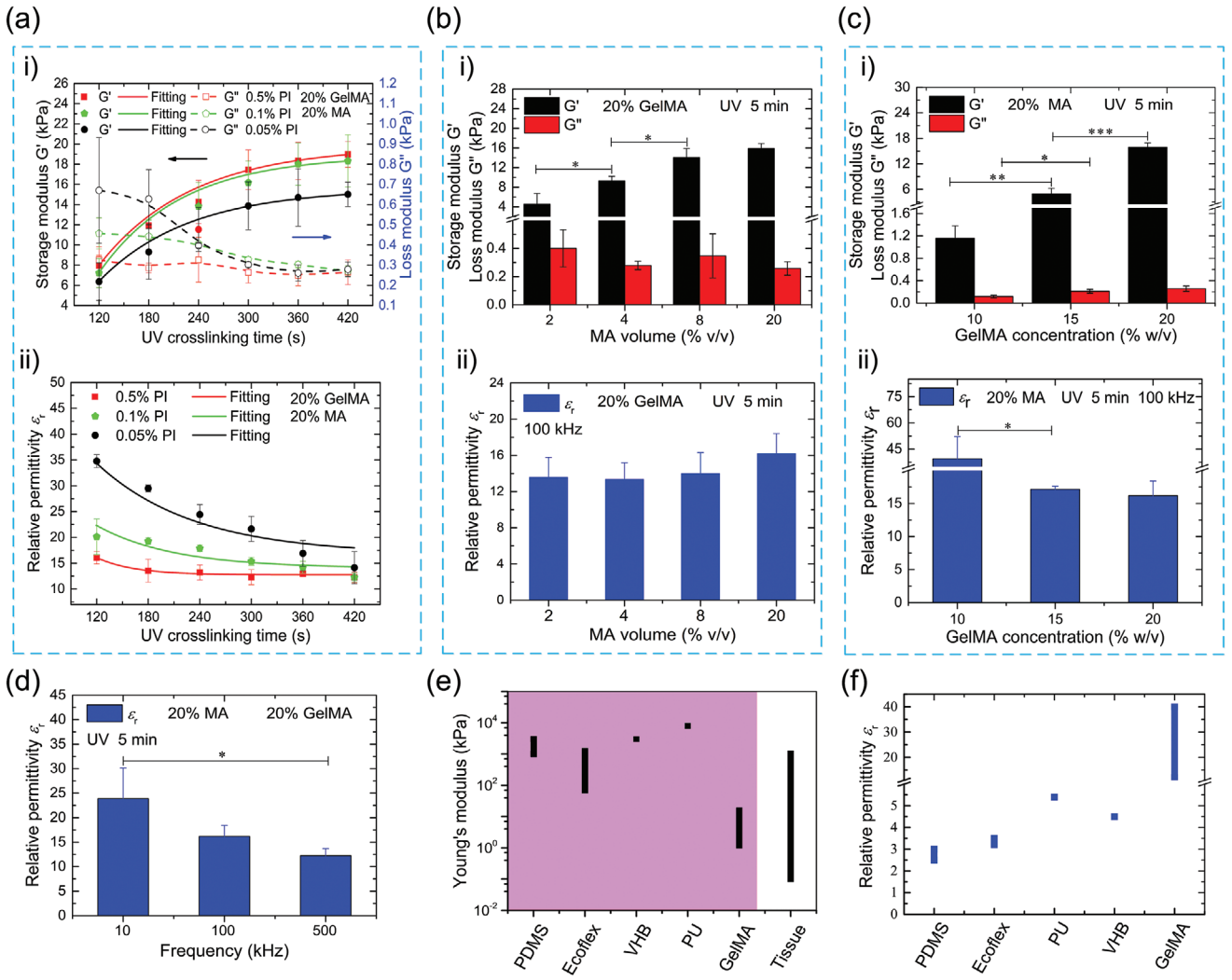

Figure 2. Mechanical and electrical properties of GelMA hydrogels under different synthesis conditions. a) The variation of the mechanical and electrical properties (relative permittivity) with UV crosslinking time. i) Variation of storage and loss modulus. ii) Variation of relative permittivity. b) Effects of MA volume (DS of MA) on the mechanical and electrical properties of GelMA hydrogels. i) Variation of the storage and loss modulus with MA volume. ii) Variation of relative permittivity with MA volume. c) Effects of GelMA concentration on the mechanical and electrical properties. i) Variation of the storage and loss modulus with GelMA concentration. ii) Variation of the relative permittivity with GelMA concentration. d) The relative permittivity of GelMA hydrogels under different frequencies. e) Comparison of Young's modulus of GelMA hydrogels with those of common elastomers. f) Comparison of the relative permittivity of GelMA hydrogels with those of common elastomers.

case, a 114% (from 0.83×10^{-3} to 1.78×10^{-3}) increase in pressure sensitivity was observed when the volume ratio of MA reduced from 20% to 2% (Figure 3c). A 40% (from 6.5×10^{-3} to 8.1×10^{-3}) increase was observed when the GelMA concentration decreased from 20% to 15% (Figure 3d). This tunability can be significantly amplified when the thickness of the GelMA dielectric layers is reduced, which is theoretically demonstrated in Figure S2c, Supporting Information. Consistent with the change in relative permittivity, the capacitance variation of the GelMA pressure sensor increased with decreased frequency (Figure 3e), suggesting another approach to tune the pressure sensitivity.[3,29] Taken together, the pressure sensitivity of GelMA hydrogel-based pressure sensors can be tuned by varying the MA volume, GelMA concentration, and working frequency.

2.3. Enabling All Solution-Processed Pressure Sensors with Microstructured GelMA Hydrogels

In the last section, we used a layer-by-layer stacked structure to evaluate the ability of GelMA hydrogels in developing highly-sensitive and performance-tunable pressure sensors. Further development of the solution-processable fabrication technique could take full advantage of the GelMA hydrogel for low-cost and large-area production. Toward this goal, we proposed a unique device structure where PDMS/GelMA/PDMS is used as a dielectric layer, and PEDOT:PSS as electrodes (**Figure 4**a). PEDOT:PSS is selected because of its solution processability, high conductivity, and transparency.[14,43–48] PDMS is employed because of its biocompatible compliance with human tissue, solution-processability, and much lower Young's modulus

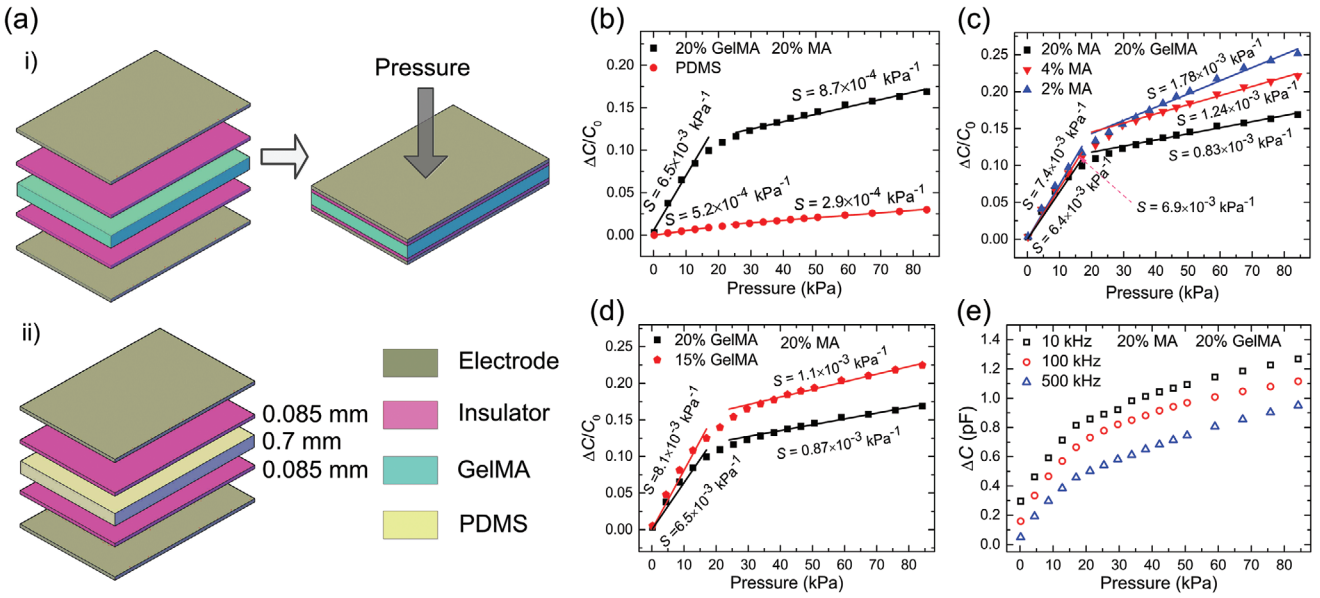

Figure 3. Schematic illustrations of stacked capacitive pressure sensors and pressure sensitivity evaluation under different synthetic conditions. a) Structure schematics of stacked pressure sensors: i) GelMA-based pressure sensors; ii) PDMS-based pressure sensors; for both types of sensors, the aluminum film, and parafilm are used as electrodes and insulation layers, respectively. b) Pressure sensitivity comparison between two types of pressure sensors. c) Variation of pressure sensitivity with MA volume (i.e., DS of MA). d) Variation of pressure sensitivity with GelMA concentration. e) Capacitance changes of GelMA-based pressure sensors under different frequencies.

than that of the widely used substrate, polyethylene terephthalate (E, ≈2.7 GPa).[49,50] GelMA is used as the core dielectric layer, and is made into pyramidal structures to improve the pressure sensitivity. The PDMS layer interposed between the GelMA and PEDOT:PSS layers has three functions: i) Acts as an insulation layer to prevent ionic conduction between the electrode and GelMA hydrogel and increase the device reproducibility;[30,51] ii) serves as an encapsulation layer to avoid the water-loss of the GelMA hydrogel; iii) allows tough interface adhesion between PDMS and GelMA when pre-treated with benzophenone solution.[52] Finally, together with the interposed PDMS, an outmost PDMS substrate layer is used to prevent possible delamination during long-term operation and conductivity deterioration of the PEDOT:PSS electrode in air and humid conditions. It should be noted that the interposed PDMS layer has a negligible effect on the device performance.[30] The working mechanism of the microstructured GelMA pressure sensor is illustrated in Figure S3, Supporting Information.

The fabrication process of the microstructured GelMA hydrogel pressure sensors began with the preparation of a PDMS mold from a silicon wafer with a pyramidal topology structure (Figure 4b-i).[6] Sequentially, the PDMS mold was immersed into a pre-heated GelMA precursor solution, followed by sonication at 37 °C to remove bubbles in the pyramidal cavities of the PDMS mold (Figure 4b-ii). Next, the PDMS mold with filled GelMA precursor was laminated to a benzophenone-treated PDMS/PEDOT: PSS/PDMS film (see Figure S4, Supporting Information, for the detailed fabrication process) under pressure, improving the structure uniformity (Figure 4b-iii). The GelMA precursor-filled PDMS mold was then exposed to UV light to partially crosslink GelMA hydrogel, and simultaneously bond the GelMA hydrogel with the PDMS/PEDOT:PSS/PDMS electrode (Figure 4b-iv). This partial crosslinking aims to increase the adhesion of the microstructured GelMA hydrogel with the other electrode. The mechanism of the bonding between PDMS and GelMA is based on the alleviation of oxygen inhibition effect and surface activation of PDMS after the treatment of benzophenone solution. The stretchy polymer networks of the pre-shaped GelMA hydrogels are grafted on PDMS by covalent crosslinking under UV light exposure, resulting in a robust interface.[52] The bonded electrode/GelMA film was peeled off (Figure 4b-v) from the PDMS mold and attached to the second benzophenone-treated PDMS/PEDOT:PSS/PDMS electrode (Figure 4b-vii). The device fabrication was completed with a final exposure to UV light, fully crosslinking the microstructured GelMA hydrogel, and increasing its bonding with both electrodes (Figure 4b-viii). The GelMA hydrogel pressure sensors fabricated using our fully solution-based process is shown in Figure 4c-i, where the microstructured GelMA hydrogel dielectric layer and silicon mold are illustrated in Figure 4c-ii,c-iii, respectively.

2.4. Performance of All Solution-Processed and Microstructured GelMA Hydrogel Pressure Sensors

Figure 5 shows the performance of our all-solution processed hydrogel pressure sensor with microstructured GelMA hydrogel dielectric layers, which have a height of 420 µm, base width of 600 µm, and spacing of 1 mm with a water content of 80%. The sensor was tested between 0 and 5 kPa, which covers the pressure range of human physiological motions such as wrist pulse and vocal cord vibration. As shown in Figure 5a, a pressure sensitivity of 0.19 kPa^{-1} was obtained between 0 and

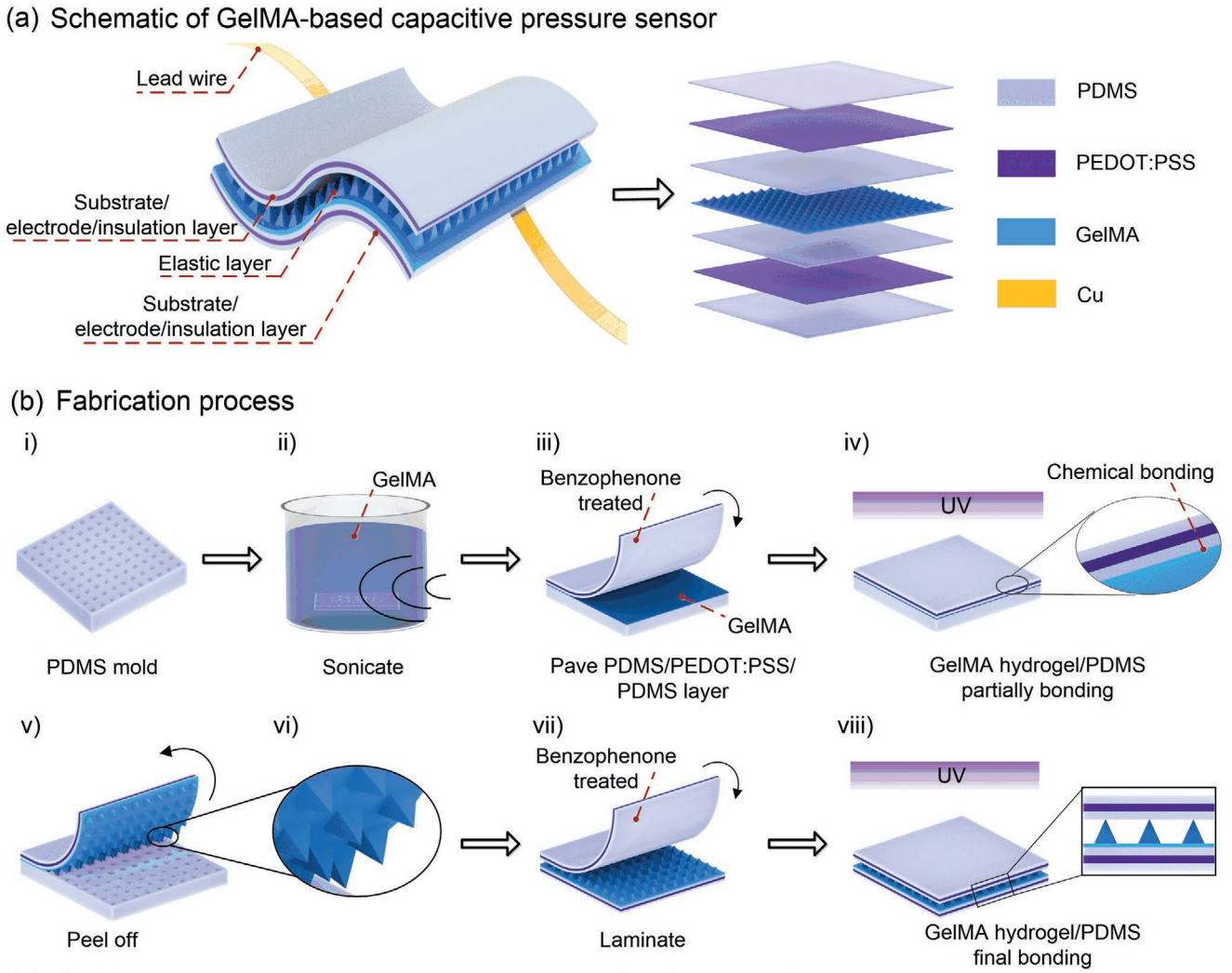

Figure 4. Schematic illustration of the structure and fabrication process of GelMA hydrogel-based pressure sensors. a) Structure schematic of the designed GelMA hydrogel-based pressure sensor. b) Fabrication process. i) Preparation of PDMS molds from a silicon wafer with pyramidal topology structure. ii) Immersing the PDMS mold into heated GelMA hydrogel precursor and sonicating to degas at 37 °C. iii) Laminating the PDMS/PEDOT:PSS/PDMS layer on the GelMA hydrogel precursor filled PDMS mold. iv) Partially UV crosslinking the GelMA hydrogel precursor to form micro pyramidal structure along with partially bonding the PDMS/PEDOT:PSS/PDMS layer with the microstructured GelMA hydrogel. v) Peeling off the PDMS/PEDOT:PSS/PDMS layer along with the microstructured GelMA hydrogel dielectric layer. vi) Zoom-in view of the GelMA hydrogel dielectric layer. vii) Laminating another PDMS/PEDOT:PSS/PDMS layer with the microstructured GelMA hydrogel dielectric layer. viii) Exposing to UV light to completely crosslink the GelMA-based pyramidal structure as well as to toughly bond it with the top and bottom PDMS/PEDOT:PSS/PDMS layers, finishing the fabrication. c) The GelMA-based pressure sensor, PDMS molds, and silicon wafer with micro pyramidal structure. i) Digital photo of a fabricated GelMA-based pressure sensor. ii,iii) SEM pictures of the GelMA hydrogel-based pyramidal structure and the silicon wafer.

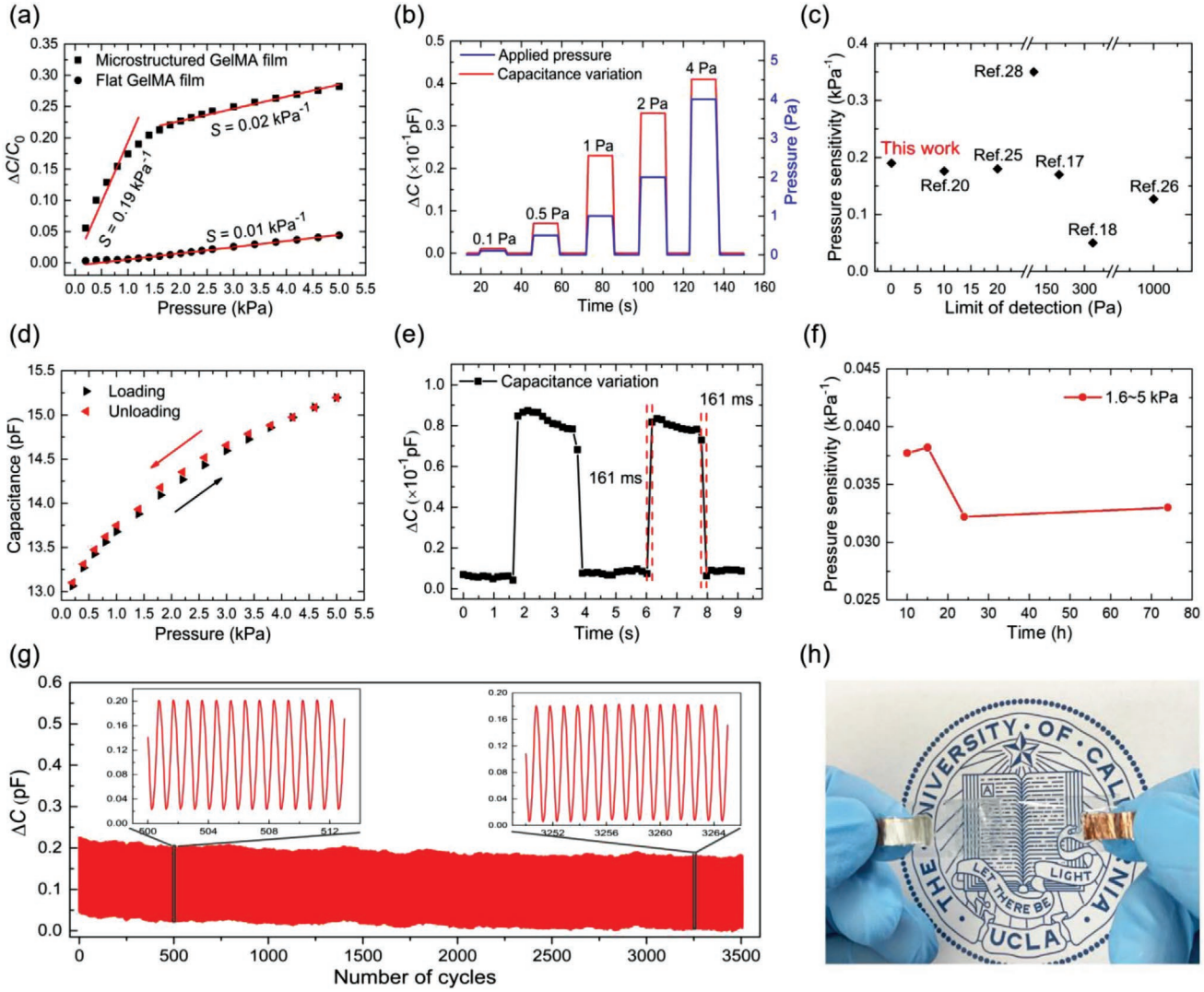

Figure 5. Performance evaluation of the fabricated microstructured GelMA hydrogel pressure sensor. a) Pressure sensitivity in the pressure range of 0–5 kPa, compared with that of the reference one based on a flat GelMA dielectric layer. b) Capacitance response under tiny pressure. c) Comparison of pressure sensitivity and LOD of this work with previously reported hydrogel pressure sensors. d) Capacitance response during loading and unloading process. e) Response time tested with a mass of 100 mg. f) Variation in pressure sensitivity with time at room temperature, from 10 to 72 h. g) Capacitance variation under a pressure of 0.5 kPa with more than 3000 times of cyclic test. h) Digital photo of the GelMA hydrogel pressure sensor with a printed badge of UCLA as background.

1.2 kPa. The pressure sensitivity was 19 times higher than that of the reference device with a flat GelMA hydrogel dielectric layer. It decreased to 0.02 kPa^{-1} when the pressure increased from 1.6 to 5 kPa, attributable to a reduced deformability of the GelMA hydrogel dielectric layer under high pressure. The LOD of our pressure senor reached as low as 0.1 Pa, which was tested with tiny weights of 1, 5, 10, 20, and 40 mg (corresponding to 0.1, 0.5, 1, 2, and 4 Pa) (Figure 5b). The pressure sensitivity of our GelMA hydrogel pressure sensors is higher, and its LOD is one order of magnitude lower than that of previously reported hydrogel pressure sensors (Figure 5c). The pressure sensitivity could be further improved by tuning the size and arrangement of the pyramid structures (see Table S1, Supporting Information, for a list of commonly used dimensions of previously reported pyramid structures).

Hysteresis is one of the factors determining the accuracy of pressure sensors, which is related to the viscoelasticity of the dielectric materials. Our GelMA pressure sensors show minimal signal variance because of the low loss modulus of GelMA hydrogel. The hysteresis was tested in the pressure range of 0 to 5 kPa analogous to wrist pulse and vocal cord vibration pressure. As shown in Figure 5d, a small hysteresis error of 4% was observed, which was much lower than that in previous reports.[53] The device showed a fast response time of ≈161 ms, both in the pressurization and relaxation process, with a weight of 100 mg (corresponding to a pressure of 10 Pa) (Figure 5e). To further evaluate the potential of the GelMA pressure sensor for practical applications, its long-term stability was investigated by exposing the device to air for 3 days. Figure 5f shows the pressure sensitivity tested at different

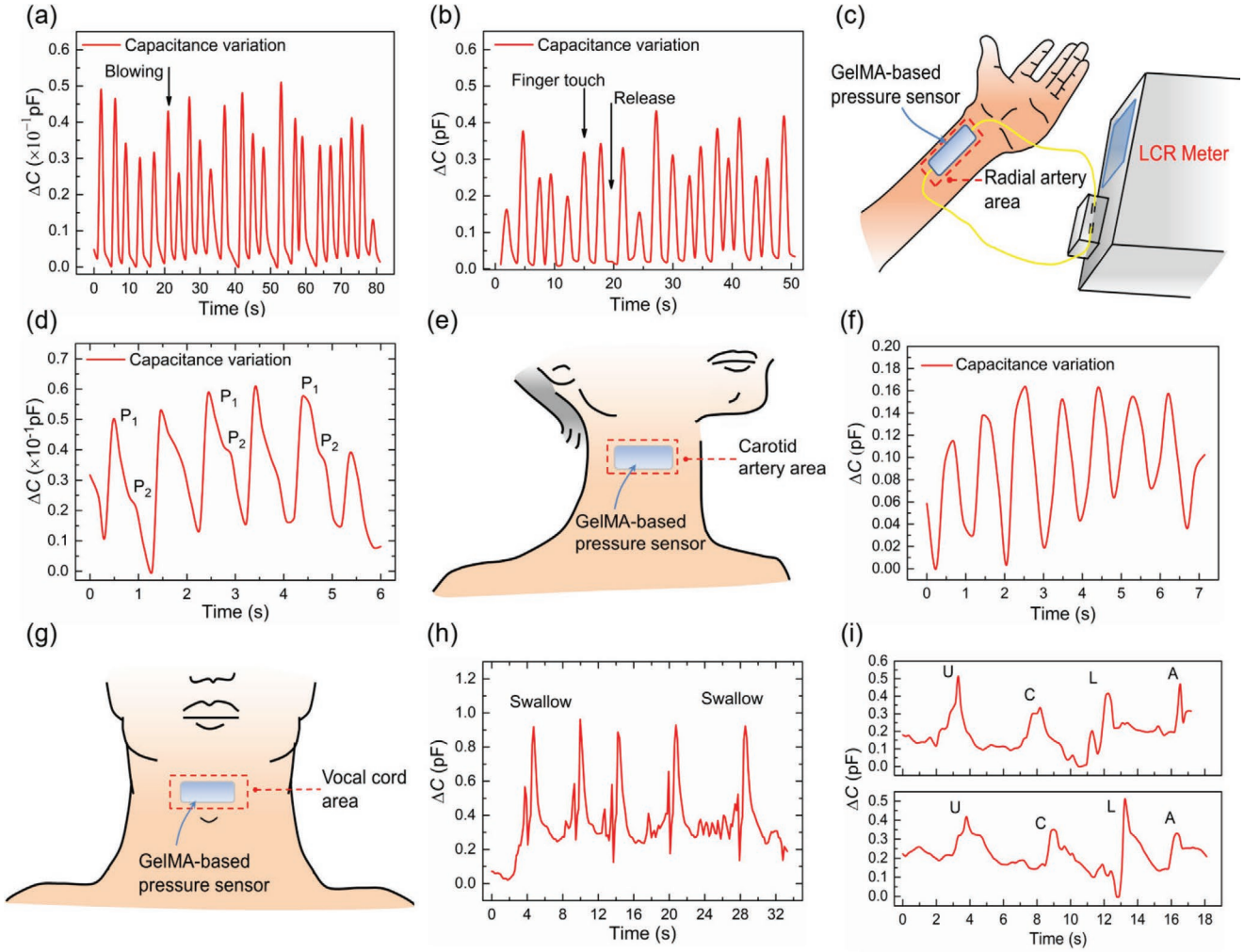

Figure 6. Applications of GelMA-based pressure sensors in monitoring of human physical or physiological signals. a) Detection of air blowing from a nitrogen gun. b) Sensing of finger touch force. c) Digital photo for set up of human wrist pulse monitoring. d) Results for wrist pulse detection. e) Schematic of the set up for carotid artery pulse measurement. f) Capacitance change with carotid artery pulse. g) Schematic of the set up for the vocal cord vibration detection. h) Capacitance change when swallowing. i) Capacitance variation when speaking letters, "U," "C," "L," and "A."

times (10, 15, 24, and 72 h). The pressure sensitivity showed a minor change of 12% (i.e., from 0.037 to 0.033 kPa^{-1}), attributable to the unique design of the PDMS/GelMA/PDMS dielectric layer where the secondary PDMS encapsulation layer could efficiently prevent water evaporation in the GelMA hydrogel. Furthermore, the device was tested for more than 3000 compression/release cycles (0–0.5 kPa), showing negligible capacitance reduction and no delamination between the GelMA-based core dielectric layer and PDMS encapsulation layer (Figure 5g). The excellent durability reflects the robustness of the chemical bonding between the PDMS and GelMA hydrogel that forms the pressure sensor.

In addition, our GelMA pressure sensors are optically transparent (Figure 5h), showing a transmittance of ≈69% at 550 nm wavelength (Figure S5, Supporting Information). This is because, during the device fabrication, all the materials selected, GelMA, PDMS, as well as the electrode PEDOT:PSS, are optically transparent. A fully transparent pressure sensor is of importance in enabling invisible wearable applications. To summarize, the small hysteresis, fast response, excellent durability, and good transparency co-demonstrate the excellence of our GelMA pressure sensor for practical wearable applications.

2.5. Applications of GelMA Hydrogel Tactile Sensors in Medical Wearables

To demonstrate the potential of our GelMA tactile sensor for practical applications, we tested the sensor under air blowing pressure and finger touch (Figure S6a,b, Supporting Information). The capacitance of the senor increased immediately in the presence of air pressure (≈0.1 kPa) and returned to its original value in the absence of the air pressure (**Figure 6**a). Similarly, the sensor was responsive to a gentle finger touch with a pressure of ≈1 kPa (Figure 6b). In both cases, the base capacitance remained stable after cyclic tests, demonstrating our GelMA-based pressure sensors have great potential to monitor the subtle pressure as wearable sensors.

The above results demonstrate the utility of our GelMA pressure sensor and encourage its application in monitoring various human physiological signals. Toward this end, the sensor was attached to different parts of the human body, the radial artery area on the wrist (Figure 6c and Figure S6c, Supporting Information), and the carotid artery area on the neck (Figure 6e and Figure S6d, Supporting Information). As shown in Figure 6c–f, the capacitance of the pressure sensor changed immediately in the presence of a pulse. Different heartbeats of 63 bpm (wrist) and 66 bpm (neck) were recorded from two volunteers. In particular, the sensor attached on the wrist can distinguish two radial artery pressure peaks, P_1 and P_2 from each pulse waveform, which are related to two crucial clinic parameters for arterial stiffness diagnosis: The radial augmentation index ($A_{Ir} = P_2/P_1$) and the time delay between P_1 and P_2 ($\Delta T_{DVP} = t_2 - t_1$). For the case tested, the A_{Ir} and ΔT_{DVP} are 66% and 486 ms, respectively, which are within the reasonable ranges of those of a volunteer.[54] These results demonstrate that the GelMA-based wearable pressure sensors are promising for healthcare applications that require real-time monitoring of physiological signals.

To further explore the potential of our GelMA pressure sensor, the device was attached to the larynx knot to examine its capability of detecting real-time swallowing and vocal cord vibration (Figure 6g and Figure S6e, Supporting Information). In the swallowing test, the capacitance showed a quick response during each swallowing activity with stable base capacitance after multiple tests (Figure 6h). In the vocal cord vibration test, the capacitance of the senor formed distinct shapes in response to different spoken words of "U," "C," "L," and "A" (Figure 6i). An identical capacitance shape was observed in the subsequent verification test, demonstrating the reliability of our sensor, and its potential for language recognition applications.

3. Conclusions

We have demonstrated the development of GelMA hydrogel-based tactile sensors for medical wearable applications. We propose a unique device structure using PDMS/GelMA/PDMS as dielectric layers and PEDOT:PSS as electrodes. This design includes four merits: i) Fully solution-processable, which allows low-cost and large-area fabrication; ii) reduced water evaporation of the GelMA hydrogel by using a PDMS encapsulation layer; iii) improved stability and device reproducibility, because of the introduction of a tough bonding method; iv) high transparency in the visible wavelength range. Our GelMA hydrogel pressure sensors show a comparable pressure sensitivity of 0.19 kPa^{-1}, and a much lower LOD of 0.1 Pa (one order of magnitude) compared with those of previous hydrogel pressure sensors because of its excellent mechanical and electrical (dielectric constant) properties. It also shows excellent durability over 3000 cycles because of the robust chemical bonding, and long-term stability up to 3 days' exposure to air due to the introduction of an PDMS encapsulation layer. These merits enable our GelMA pressure sensor to be capable of monitoring human physiological signals, demonstrating its great potential for medical wearables.

4. Experiment Section

Synthesis of GelMA: GelMA was synthesized using the procedure as described previously.[23] First, 10 g gelatin from porcine skin was added to 100 mL of Dulbecco's phosphate buffered saline (DPBS) (GIBCO) preheated at 50 °C. The mixture was stirred at 50 °C until the gelatin was completely dissolved. Sequentially, a certain volume of mythacrylic anhydride (MA) (Sigma-Aldrich) was added to the gelatin solution, stirring at 50 °C to react for 2 h. Then, the reaction was stopped by adding another preheated 100 mL of DPBS at 50 °C. Next, the mixture solution was dialyzed at 40 °C using dialysis tubing (12–14 kDa) in distilled water for at least 5 days to remove methacrylic acid and other impurities such as salt. After dialysis, the resulting clear solution was freeze-dried for at least 5 days to form porous foam and stored at −80 °C for further use. Herein, four types of volumes of MA, 20, 8, 4, and 2 mL, were added to the 100 mL of gelatin solution to synthesize GelMA with different DS of MA. The DS for the synthesized GelMA with MA volume ratios of 20% (ultra-GelMA), 8% (high-GelMA), 4% (media-GelMA), and 2% (low-GelMA), are about 85%, 75%, 60%, and 40%, respectively.[35,55]

Preparation of GelMA Hydrogel Samples: GelMA hydrogel precursors were synthesized by dissolving solid GelMA into distilled ionic (DI) water at 80 °C for 20 min after the addition of photoinitiator (Irgacure 2959). The GelMA hydrogel samples for electrical properties testing were prepared by pouring the warm GelMA hydrogel precursor into a 2 cm × 2 cm × 1cm PDMS mold with a glass placed on the top and exposing it to a UV light of 45 mW cm^{-2} for a given period. An 8 mm circular film was punched after UV crosslinking for further mechanical property testing. The GelMA hydrogel samples for the electrical properties testing were prepared directly with the PDMS mold.

Mechanical and Electrical Property Characterization of GelMA Hydrogels: The mechanical properties, such as the storage (elastic) modulus and loss (viscous) modulus, of GelMA hydrogel were tested using a Rheometer (MCR 301, Anton Paar). Oscillatory measurements were performed at 1% strain, constant frequency (1 Hz), and room temperature (25 °C). 20 points were obtained for each sample, and the averaged value was used as the final result. For the electrical property characterization, the crosslinked 2 cm × 2 cm × 1cm hydrogel films were sandwiched by two self-made electrodes to form a parallel capacitor (see Figure S7, Supporting Information, for the sandwiched structure). A LCR meter (E4980AL, Keysight Technologies) was used to measure its capacitances. The relative permittivity of GelMA hydrogel was calculated by the relationship of permittivity with capacitance (see Equation S4, Supporting Information).

Preparation and Testing of Layer-by-Layer Stacked Pressure Sensors: Two types of simply stacked pressure sensors were prepared: One with GelMA as dielectric layers (Figure 3a-i), and the reference one with PDMS as dielectric layers (Figure 3a-ii). As shown in Figure 3a, the aluminum film was used as the electrodes, and parafilm was used as the insulation layer between the aluminum film and GelMA dielectric layer because GelMA hydrogel is electrically conductive. The aluminum film, parafilm, and middle dielectric layer were stacked together to form the pressure sensor. All dimensions of the GelMA-based pressure sensor are the same as those of the PDMS-based pressure sensor. The thicknesses of the dielectric layer and parafilm are 0.7 and 0.085 mm, respectively. The area of each layer was the same as being: 10 mm × 10 mm. The stacked pressure sensor was tested at a preload of 4 kPa, which aimed to reduce the air gap between different layers and to make their structure compact. For each set of conditions, three sensors were tested, and the mean value was used as the final result.

GelMA-based dielectric layers were prepared by pouring heated GelMA hydrogel precursor into PDMS molds with a glass slide placed on the top and exposing them to UV light for 5 min. PDMS dielectric layers were made by spinning 10:1 (silicone base to the cure agent ratio) PDMS mixture on glass slides and curing at 80 °C oven for 2 h.

Preparation of Silicon Mold: A 0.5 mm thick [100] silicon wafer with 100 nm thick Si_3N_4 on both sides was used to prepare the mold. Photolithography was performed after SPR 700 photoresist was spin-coated on top of the wafer for patterning. Reactive ion etching was then performed to remove the Si_3N_4 and expose the Si. Then the wafer was immersed in 30% potassium hydroxide solution to etch away the

exposed Si part with Si_3N_4 as the etching mask. Finally, the silicon wafer with recessed micro pyramidal structures was cleaned sequentially with acetone and alcohol for future use.

Fabrication of PDMS Mold: The PDMS mold was made using a similar procedure as reported in ref. [6]. A 5:1 mixture of PDMS base to crosslinker (Sylgard 184, Dow Corning) was mixed by adequately stirring and degassing in a vacuum chamber until all air bubbles disappeared. Next, the degassed mixture was poured on the silicon mold, degassed again, and cured at 80 °C for at least 4 h. Sequentially, the cured PDMS was cut off to form the first inverted mold, and then treated with a spin-coated layer of cetyltrimethylammoniumbromide (CTAB) solution and dried in an 80 °C oven. Then, the final PDMS mold was made based on the first inverted mold with an identical procedure.

PEDOT:PSS Mixture Preparation: PEDOT:PSS (Clevios PH1000 from Heraeus Electronic Materials) solution was obtained by adding 5 v/v% of glycerol, 0.2 v/v% of 3-glycidoxypropyltrimethoxysilane, and 1v/v% of capstone. The mixture was sonicated for 20 min and then filtered with 0.45 µm syringe filters for further use.

Fabrication and Characterization of PDMS/PEDOT:PSS/PDMS Film: The fabrication process of PDMS/PEDOT:PSS/PDMS film started with a 10:1 mixture of PDMS base (Sylgard 184, Dow Corning) to crosslinker mixed by adequately stirring and degassing in a vacuum chamber until all air bubbles disappeared. The mixture was spin-coated on a pre-treated glass with CTAB solution at 2000 rpm, and then cured at 80 °C for 2 h (Figure S4a, Supporting Information). The cured PDMS film was cleaned with isopropanol for 30 s, dried with a nitrogen gun, and then treated with oxygen plasma etch for 2 min. Immediately after, PEDOT:PSS solution was spin-coated on the PDMS film at 1000 rpm, and cured on a hotplate at 160 °C for 50 min (Figure S4b, Supporting Information). Once cured, the copper lead wire was attached to the PEDOT:PSS film with conductive sliver glue and annealed at 100 °C for 2 h to reduce the contact resistance between them (not shown in the schematic). Next, another PDMS film was spin-coated on the PEDOT:PSS layer at 1500 rpm and cured at 80 °C for 2 h again (Figure S4c, Supporting Information). Once cured, the PDMS/PEDOT:PSS/PDMS film was carefully peeled off from the glass slides, thoroughly cleaned with methanol, and completely dried with a nitrogen gun (Figure S4d, Supporting Information). It was further treated with benzophenone solution (10 w/v% in ethanol) for 5 min at room temperature, and washed with methanol, and dried by nitrogen again for further bonding with microstructured GelMA hydrogel dielectric layer (Figure S4f, Supporting Information). The thicknesses of the PDMS/PEDOT:PSS/PDMS films are 40 um/10 um/60 um, respectively, which were tested using Dektak 150 Surface Profiler (Veeco Instruments Inc., USA).

Bonding of the GelMA Hydrogel Dielectric Layer with the PDMS/PEDOT:PSS/PDMS Film: During the fabrication process of the GelMA-based pressure sensors, two UV crosslinking steps were used. The first step to partially bond the GelMA hydrogel and PDMS was conducted by exposing the device to 45 mW cm^{-2} of UV light for about 50 s for microstructured GelMA hydrogel dielectric layers and 30 s for the reference flat GelMA dielectric layer. The final crosslinking step was implemented by exposing the device to UV light for 5 min under the same UV light strength. The exposed edges of the fabricated GelMA pressure sensors were sealed with glue.

Performance Testing of All Solution-Processed GelMA Pressure Sensors: An Instron (5900 Series) with a force resolution of 1×10^{-4} N was used to apply pressure. The force and displacement of the test head can be accurately controlled by a computer. When testing, a glass (10 mg) with a size of 10 mm × 10 mm was placed on the tested sensor for uniform pressure. The capacitance was measured using LCR meter (E4980AL, Keysight Technologies) at 100 kHz with a 1 V AC signal unless otherwise specified. The transparency of the GelMA pressure sensor was tested by Hitachi U-4100 spectrophotometer with an integrating sphere equipped.

Institutional Review Board Approval for Human Subject Testing: The conducted human subject experiments were performed in compliance with the protocols that have been approved by the Institutional Review Board (IRB) at the University of California, Los Angeles (IRB#17-000170). All subjects gave written informed consent before participation in the study. For all demonstrations on human skin, signed consent was obtained from the volunteer.

Supporting Information

Supporting Information is available from the Wiley Online Library or from the author.

Acknowledgements

The authors acknowledge the Integrated Systems Nanofabrication Cleanroom (ISNC) in California NanoSystems Institute (CNSI). This work was supported by the National Institutes of Health (1R01HL140951-01A1, 1R01GM126571-01, 1R01GM126831-01, 1R01EB023052-01A1), the National Natural Science Foundation of China (51805423, 51875449, 91748207, 51421004), and the International Postdoctoral Exchange Fellowship Program (20180067).

Conflict of Interest

The authors declare no conflict of interest.

Keywords

gelatin methacryloyl hydrogels, healthcare, interface adhesion, PEDOT:PSS, solution-processable, transparent devices, wearable tactile sensors

Received: April 24, 2020
Revised: June 23, 2020
Published online: September 6, 2020

[1] M. Chu, T. Nguyen, V. Pandey, Y. Zhou, H. N. Pham, R. Bar-Yoseph, S. Radom-Aizik, R. Jain, D. M. Cooper, M. Khine, *npj Digital Med.* **2019**, *2*, 8.
[2] Y. J. C. Kenry, C. T. Lim, *Microsyst. Nanoeng.* **2016**, *2*, 1.
[3] Y. Huang, X. Fan, S.-C. Chen, N. Zhao, *Adv. Funct. Mater.* **2019**, *29*, 1808509.
[4] T. Yang, D. Xie, Z. Li, H. Zhu, *Mater. Sci. Eng., R* **2017**, *115*, 1.
[5] Y. Khan, A. E. Ostfeld, C. M. Lochner, A. Pierre, A. C. Arias, *Adv. Mater.* **2016**, *28*, 4373.
[6] B. C.-K. Tee, A. Chortos, R. R. Dunn, G. Schwartz, E. Eason, Z. Bao, *Adv. Funct. Mater.* **2014**, *24*, 5427.
[7] X. Y. Yin, Y. Zhang, X. Cai, Q. Guo, J. Yang, Z. L. Wang, *Mater. Horiz.* **2019**, *6*, 767.
[8] D. Kwon, T.-I. Lee, J. Shim, S. Ryu, M. S. Kim, S. Kim, T.-S. Kim, I. Park, *ACS Appl. Mater. Interfaces* **2016**, *8*, 16922.
[9] C. Mu, J. Li, Y. Song, W. Huang, A. Ran, K. Deng, J. Huang, W. Xie, R. Sun, H. Zhang, *ACS Appl. Nano Mater.* **2018**, *1*, 274.
[10] T. Li, H. Luo, L. Qin, X. Wang, Z. Xiong, H. Ding, Y. Gu, Z. Liu, T. Zhang, *Small* **2016**, *12*, 5042.
[11] Y. Wan, Z. Qiu, Y. Hong, Y. Wang, J. Zhang, Q. Liu, Z. Wu, C. F. Guo, *Adv. Electron. Mater.* **2018**, *4*, 1700586.
[12] Q. J. Sun, X.-H. Zhao, Y. Zhou, C.-C. Yeung, W. Wu, S. Venkatesh, Z.-X. Xu, J. J. Wylie, W.-J. Li, V. A. L. Roy, *Adv. Funct. Mater.* **2019**, *29*, 1808829.
[13] H. Yuk, B. Lu, X. Zhao, *Chem. Soc. Rev.* **2019**, *48*, 1642.
[14] Y. Liu, J. Liu, S. Chen, T. Lei, Y. Kim, S. Niu, H. Wang, X. Wang, A. M. Foudeh, J. B.-H. Tok, Z. Bao, *Nat. Biomed. Eng.* **2019**, *3*, 58.
[15] M.-J. Yin, Z. Yin, Y. Zhang, Q. Zheng, A. P. Zhang, *Nano Energy* **2019**, *58*, 96.
[16] J. Huang, M. Zhao, Y. Cai, M. Zimniewska, D. Li, Q. Wei, *Adv. Electron. Mater.* **2020**, *6*, 1900934.
[17] Z. Lei, Q. Wang, S. Sun, W. Zhu, P. Wu, *Adv. Mater.* **2017**, *29*, 1700321.

[18] G. Ge, Y. Zhang, J. Shao, W. Wang, W. Si, W. Huang, X. Dong, *Adv. Funct. Mater.* **2018**, *28*, 1802576.
[19] M.-j. Yin, Y. Zhang, Z. Yin, Q. Zheng, A. P. Zhang, *Adv. Mater. Technol.* **2018**, *3*, 1800051.
[20] Y. Tai, M. Mulle, I. A. Ventura, G. Lubineau, *Nanoscale* **2015**, *7*, 14766.
[21] Y. Zhu, W. Lu, Y. Guo, Y. Chen, Y. Wu, H. Lu, *RSC Adv.* **2018**, *8*, 36999.
[22] P. Chakraborty, T. Guterman, N. Adadi, M. Yadid, T. Brosh, L. Adler-Abramovich, T. Dvir, E. Gazit, *ACS Nano* **2019**, *13*, 163.
[23] K. Yue, G. Trujillo-De Santiago, M. M. Alvarez, A. Tamayol, N. Annabi, A. Khademhosseini, *Biomaterials* **2015**, *73*, 254.
[24] D. Loessner, C. Meinert, E. Kaemmerer, L. C. Martine, K. Yue, P. A. Levett, T. J. Klein, F. P. W. Melchels, A. Khademhosseini, D. W. Hutmacher, *Nat. Protoc.* **2016**, *11*, 727.
[25] Z. Wang, Y. Si, C. Zhao, D. Yu, W. Wang, G. Sun, *ACS Appl. Mater. Interfaces* **2019**, *11*, 27200.
[26] Z. Qin, X. Sun, Q. Yu, H. Zhang, X. Wu, M. Yao, W. Liu, F. Yao, J. Li, *ACS Appl. Mater. Interfaces* **2020**, *12*, 4944.
[27] X. Xia, X. Zhang, M. J. Serpe, Q. Zhang, *Adv. Mater. Technol.* **2019**, *5*, 2070011.
[28] J. Duan, X. Liang, J. Guo, K. Zhu, L. Zhang, *Adv. Mater.* **2016**, *28*, 8037.
[29] G. Schwartz, B. C.-K. Tee, J. Mei, A. L. Appleton, D. H. Kim, H. Wang, Z. Bao, *Nat. Commun.* **2013**, *4*, 1859.
[30] S. R. A. Ruth, L. Beker, H. Tran, V. R. Feig, N. Matsuhisa, Z. Bao, *Adv. Funct. Mater.* **2019**, *30*, 1903100.
[31] A. I. V. D. Bulcke, B. Bogdanov, N. D. Rooze, E. H. Schacht, M. Cornelissen, H. Berghmans, *Biomacromolecules* **2000**, *1*, 31.
[32] C. D. O'connell, B. Zhang, C. Onofrillo, S. Duchi, R. Blanchard, A. Quigley, J. Bourke, S. Gambhir, R. Kapsa, C. Di Bella, P. Choong, G. G. Wallace, *Soft Matter* **2018**, *14*, 2142.
[33] M. Sun, X. Sun, Z. Wang, S. Guo, G. Yu, H. Yang, *Polymers* **2018**, *10*, 1290.
[34] X. Zhao, Q. Lang, L. Yildirimer, Z. Y. Lin, W. Cui, N. Annabi, K. W. Ng, M. R. Dokmeci, A. M. Ghaemmaghami, A. Khademhosseini, *Adv. Healthcare Mater.* **2016**, *5*, 108.
[35] J. W. Nichol, S. T. Koshy, H. Bae, C. M. Hwang, S. Yamanlar, A. Khademhosseini, *Biomaterials* **2010**, *31*, 5536.
[36] D. Buenger, F. Topuz, J. Groll, *Prog. Polym. Sci.* **2012**, *37*, 1678.
[37] J. Heikenfeld, A. Jajack, J. Rogers, P. Gutruf, L. Tian, T. Pan, R. Li, M. Khine, J. Kim, J. Wang, J. Kim, *Lab Chip.* **2018**, *18*, 217.
[38] Z. Wen, J. Yang, H. Ding, W. Zhang, D. Wu, J. Xu, Z. Shi, T. Xu, Y. Tian, X. Li, *J. Mater. Sci.: Mater. Electron.* **2018**, *29*, 20978.
[39] H. Xia, M. Song, *J. Mater. Chem.* **2006**, *16*, 1843.
[40] J. Wang, J. Jiu, M. Nogi, T. Sugahara, S. Nagao, H. Koga, P. He, K. Suganuma, *Nanoscale* **2015**, *7*, 2926.
[41] P. Brochu, Q. Pei, *Macromol. Rapid Commun.* **2010**, *31*, 10.
[42] T. G. McKay, E. Calius, I. A. Anderson, presented at the Electroactive Polymer Actuators and Devices (EAPAD) 2009, San Diego, CA, March **2009**.
[43] L. V. Kayser, D. J. Lipomi, *Adv. Mater.* **2019**, *31*, 1806133.
[44] H. Shi, C. Liu, Q. Jiang, J. Xu, *Adv. Electron. Mater.* **2015**, *1*, 1500017.
[45] N. Kim, S. Kee, S. H. Lee, B. H. Lee, Y. H. Kahng, Y.-R. Jo, B.-J. Kim, K. Lee, *Adv. Mater.* **2014**, *26*, 2268.
[46] D. J. Lipomi, J. A. Lee, M. Vosgueritchian, B. C.-K. Tee, J. A. Bolander, Z. Bao, *Chem. Mater.* **2012**, *24*, 373.
[47] S. Zhang, H. Ling, Y. Chen, Q. Cui, J. Ni, X. Wang, M. C. Hartel, X. Meng, K. Lee, J. Lee, W. Sun, H. Lin, S. Emaminejad, S. Ahadian, N. Ashammakhi, M. R. Dokmeci, A. Khademhosseini, *Adv. Funct. Mater.* **2019**, *30*, 1906016.
[48] S. Zhang, Y. Chen, H. Liu, Z. Wang, H. Ling, C. Wang, J. Ni, B. Çelebi-Saltik, X. Wang, X. Meng, H.-J. Kim, A. Baidya, S. Ahadian, N. Ashammakhi, M. R. Dokmeci, J. Travas-Sejdic, A. Khademhosseini, *Adv. Mater.* **2020**, *32*, 1904752.
[49] Y. Mi, Y. Chan, D. Trau, P. Huang, E. Chen, *Polymer* **2006**, *47*, 5124.
[50] S. Y. Hong, Y. H. Lee, H. Park, S. W. Jin, Y. R. Jeong, J. Yun, I. You, G. Zi, J. S. Ha, *Adv. Mater.* **2016**, *28*, 930.
[51] S. Ahadian, J. Ramon-Azcon, M. Estili, X. Liang, S. Ostrovidov, H. Shiku, M. Ramalingam, K. Nakajima, Y. Sakka, H. Bae, T. Matsue, A. Khademhosseini, *Sci. Rep.* **2014**, *4*, 4271.
[52] H. Yuk, T. Zhang, G. A. Parada, X. Liu, X. Zhao, *Nat. Commun.* **2016**, *7*, 12028.
[53] L. Pan, A. Chortos, G. Yu, Y. Wang, S. Isaacson, R. Allen, Y. Shi, R. Dauskardt, Z. Bao, *Nat. Commun.* **2014**, *5*, 3002.
[54] W. Nichols, *Am. J. Hypertens.* **2005**, *18*, 3S.
[55] H. Shin, B. D. Olsen, A. Khademhosseini, *Biomaterials* **2012**, *33*, 3143.